Effect of Silicon Content on the Microstructure and Mechanical Properties of TiAlSiN Coatings Prepared by Reactive Magnetron Sputtering

Xudong Sui[1], Guojian Li[*2], Qiang Wang[3], Huan Qi[4], Xiangkui Zhou[5], Kai Wang[6]

[1-6]Key Laboratory of Electromagnetic Processing of Materials, Northeastern University, Shenyang 110819, China

[1]suixud@126.com; [*2]gjli@epm.neu.edu.cn; [3]wangq@mail.neu.edu.cn

***Abstract*-Titanium Aluminum Silicon Nitride (TiAlSiN) coating has been expected to be applied in the field of cutting new difficult-to-machine materials such as titanium and superalloys. TiAlSiN coatings in the range of 4-8 at.% silicon content are prepared by reactive magnetron sputtering. The results show that the structure of nanocrystal surrounded by amorphous Si_3N_4 was formed in all the TiAlSiN coatings. When the silicon content increases to 8 at.%, the grain size of TiAlSiN coatings is refined to 7 nm and distributes in a narrow size range. Meanwhile, the nano-column growth of the TiAlSiN coating with 4 at.% silicon disappeared and changed to nanocrystals growth. The hardness as a function of the silicon content showed a nonlinear relationship, and the highest hardness is obtained at 6 at.% silicon content. TiAlSiN coating with 4 at.% silicon content has the highest critical load of 87.8 N. With increasing silicon content, the preferred orientations change from (111) to (200) and the adhesion strength decreased. The optimized mechanical properties of the TiAlSiN coatings, with a hardness of about 32.8 GPa and a critical load of 69.2 N, will have a promising application in modern cutting technology.**

Keywords- Sputtering; TiAlSiN Coatings; Microstructure; Nanocomposite; Nanoindentation; Adhesion

I. INTRODUCTION

Hard coatings have shown particularly promising for cutting operations [1, 2]. However, the development of high speed and dry cutting technology puts forward new requirements to the performance of cutting tool [3, 4]. One of the most used solutions is to add substitutional elements such as silicon, chromium and carbon into the traditional transition metal nitride coatings to form nanocomposite coatings [5-8] Since TiAlSiN (Titanium Aluminum Silicon Nitride) nanocomposite coatings can form a structure of nanocrystallines embedded in an amorphous phase, which can result in high hardness and excellent thermal stability [9-11], it is expected to be used in modern cutting.

Previous studies on TiAlSiN coatings mostly used are ion plating technology [12, 13], TiAlSiN coatings prepared by magnetron sputtering were reported relatively less. However, magnetron sputtering can avoid the large particles, thereby obtaining a good quality and excellent mechanical properties coating [14]. Moreover, former works on TiAlSiN coatings are mostly about the preparation condition, microstructure and hardness. The effect of changes in microstructure on the mechanical properties after the introduction of silicon element is a complex issue not well understood. In this work, TiAlSiN coatings were prepared by magnetron sputtering method and the relationship between microstructure and mechanical properties of TiAlSiN coatings was fully discussed. Two or more alloy targets are usually used to prepare quaternary TiAlSiN coatings, but in this work a single TiAlSi alloy target is used to prepare TiAlSiN coatings, so as to simplify operations and improve productivity.

II. MATERIALS AND METHODS

The TiAlSiN coatings were prepared on cemented carbide substrates using reactive magnetron sputtering method. The substrates were first polished with diamond abrasive discs, and then with diamond pastes of 2.5 μm, until smooth surfaces with a roughness of Rq = 10 nm were obtained. Then, substrates were cleaned with acetone and ethanol in an ultrasonic cleaner, respectively.

Sputtering was conducted on a multifunctional coating machine, as shown in Fig. 1, under a base vacuum level with pressure $\leq 3\times10^{-3}$ Pa. Pure titanium (99.9%) and TiAlSi alloy targets (titanium and aluminum atomic ratio is 5:4, but change the content of silicon: 4, 6 and 8 at. %) were tested during this study. The targets were cleaned by sputtering in argon gas for 5 min before depositing coatings. A titanium buffer layer about 300 nm thick was deposited preferentially to increase the adhesion force between substrate and coating the main coating process parameters are shown in Table 1.

DOI: 10.5963/AMSA0401001

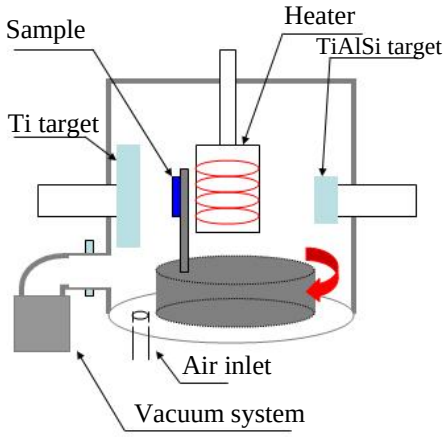

Fig. 1 Schematic diagram of the experimental apparatus

TABLE 1 DEPOSITION PARAMETERS

Layer	Ti	TiAlSiN
Ar pressure (Pa)	0.3	0.3
N_2 pressure (Pa)	---	0.08
Power (W)	1440	700
Temperature (^oC)	350	350
Deposition times (min)	5	60
Target	Titanium (99.9%)	Silicon content =4 at.%, 6 at.%, 8 at.%

The morphology and thickness of TiAlSiN coatings were characterized by a scanning electron microscope (SEM, SUPRA 35). The content of coatings is determined by using an energy dispersive spectroscopy (EDS). The structures were characterized by a glazing incidence X-ray diffraction (GIXRD, D/MAX 2400) with an incident angle of 1^o. The microstructure was determined by transmission electron microscopy (TEM, Tecnai G2 F30); whereas the chemical bonding of TiAlSiN coatings was determined by an X-ray photoelectron spectroscopy (XPS, ESCALAB250). A G200 nanoindenter was used to measure the hardness and elastic modulus with the indentation depth of approximately 250 nm. The critical adhesion strength was measured with an automatic scratch tester.

III. RESULTS AND DISCUSSION

A. Buffer Layer

Although the interface problem between coating and substrate has a significant effect on cutting efficiency, many studies have shown that the buffer layer is an effective method to solve bond strength of coating and substrate [6, 12, 13]. Since titanium has a good wettability with cemented cabide and also a good affinity to transition metal nitride coatings [15], a titanium buffer layer about 300 nm was deposited firstly to increase adhesion strength in this study. Adhesion strength of TiAlN (Titanium Aluminum Nitride) coatings with and without a titanium buffer layer was tested and the results are shown in Fig. 2. The comparison of these results indicates that TiAlN coating with a titanium buffer layer has a better adhesion strength than that without a buffer layer.

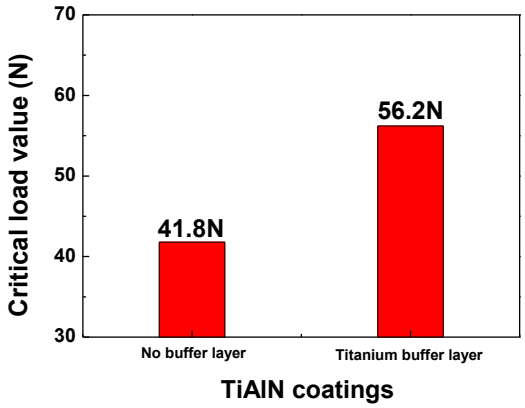

Fig. 2 Critial load values of TiAlN coatings prepared with and without Titanium buffer layer

DOI: 10.5963/AMSA0401001

B. Composition and Structure

Since the nitrogen element cannot be accurately detected by EDS, this study only discussed the relative contents of titanium, aluminum and silicon, as shown in Table 2; where S1, S2 and S3 refer to sample 1, sample 2 and sample 3, respectively. They were prepared using TiAlSi alloy targets with 4 at.%, 6 at.% and 8 at.% silicon content, respectively.

TABLE 2 CONTENTS OF TIALSIN COATINGS DETECTED BY EDS

Sample	Ti at.%	Al at.%	Si at.%
S1	52.1	44.1	3.8
S2	50.0	44.4	5.6
S3	50.0	42.1	7.9

The XRD diffraction peaks of TiAlSiN coatings are displayed in Fig. 3. The dash line in Fig. 3 represents the standard XRD pattern of NaCl-structure TiAlN. All peaks of TiAlSiN coatings were shown to be the NaCl structure of TiAlN phase. In addition, there were no peaks related with nitrides of Al and Si. With increasing silicon content, the preferred orientations changed from (111) to (200). Moreover, the peak (111) intensity decreased sharply, which may result from the formation of nanocrystal or amorphous phase. The results obtained were consistent with the results published elsewhere [12, 13, 16]. Furthermore, the diffraction peaks are also considerably broadened with increasing silicon content, which means that the grain size decreased [17] or the amorphous phase began to form.

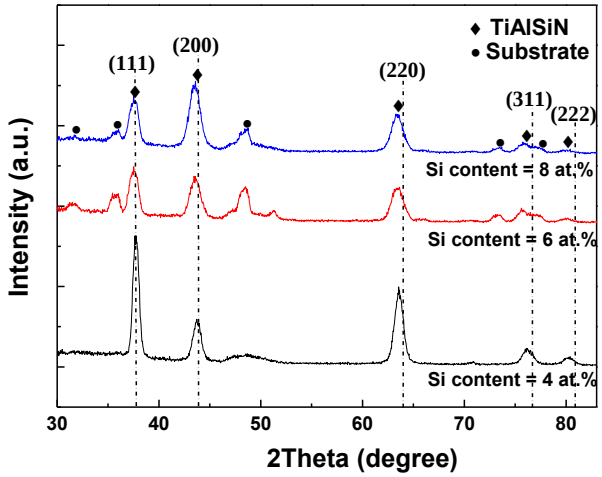

Fig. 3 XRD patterns of different TiAlSiN films prepared with different silicon contents: (a) silicon content = 4 at.%, (b) silicon content = 6 at.%, (c) silicon content = 8 at.%. The dash lines are the standard peaks of NaCl-structure TiAlN

In addition, XPS was brought to characterize the chemical bonding state of N (nitrogen) and Si (silicon) in order to determine whether there is amorphous Si_3N_4 in the coatings. The corresponding results are shown in Figs. 4 and 5. Two peaks, which are near 396.0 eV and 398.9 eV appeared in the N 1s spectrum. The peak near 396.0 eV is derived from AlN (Aluminum nitride) or TiN (Titanium Nitride). The peak at 398.9 eV is derived from nitrogen in Si_3N_4.

It can be seen from Fig. 5 that one peak was located near about 101-102 eV in silicon 2p spectrum, which is close to the reference value of Si_3N_4. Thus, the TiAlSiN coating is proved to be composed by nanocrystalline TiAlN or TiAlSiN and amorphous Si_3N_4 according to XRD and XPS results.

DOI: 10.5963/AMSA0401001

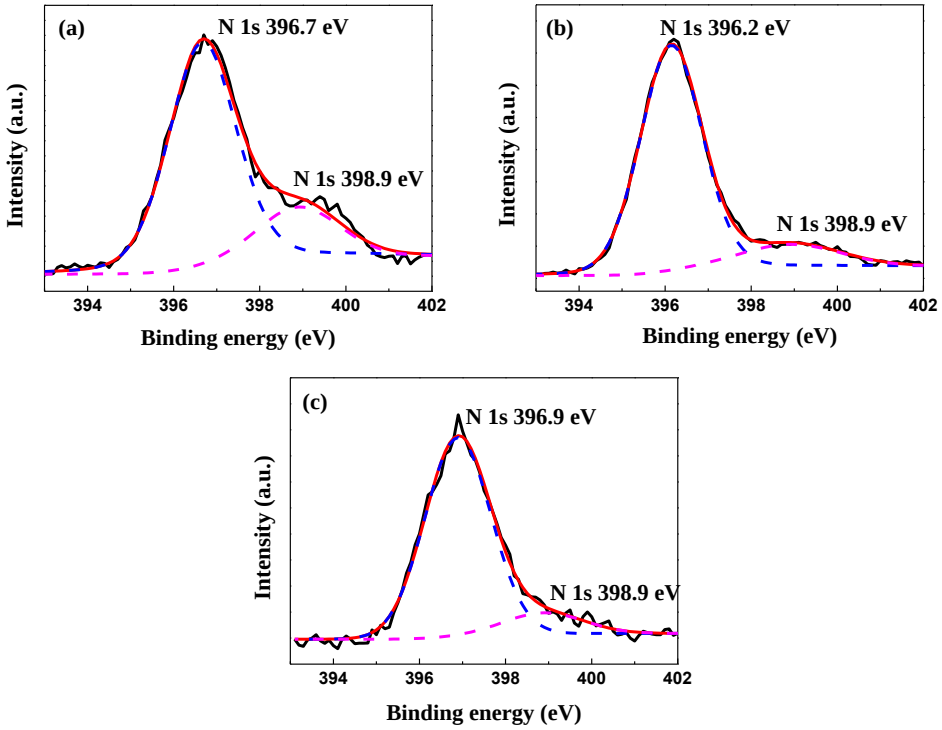

Fig. 4 XPS spectra of N 1s peaks for the TiAlSiN coatings with different silicon contents: (a) silicon content = 4 at.% (b) silicon content = 6 at.%, (c) silicon content = 8 at.%

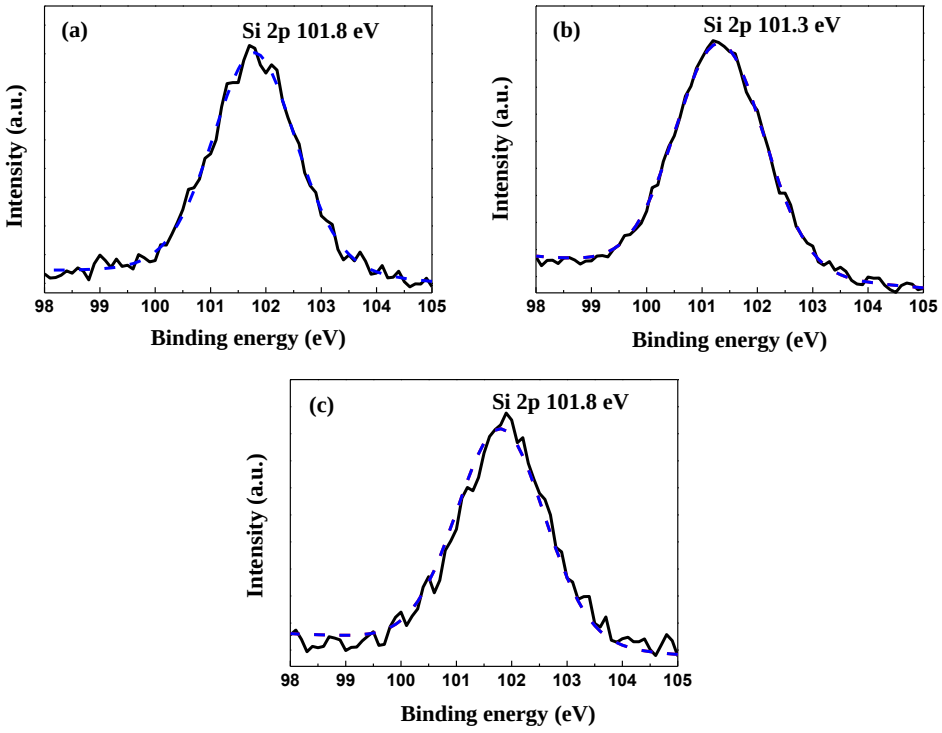

Fig. 5 XPS spectra of silicon 2p peaks for the TiAlSiN coatings with different silicon contents: (a) silicon content = 4 at.%, (b) silicon content = 6 at.%, (c) silicon content = 8 at.%

C. Morphology and Grain Size

Fig. 6 shows that the surface topography changes with increasing silicon content. From Figs. 6(a)-6(c), a denser and finer film was obtained with increasing silicon content from 4 at.% to 8 at.%. Furthermore, some spherical clusters appear on the surface of TiAlSiN coatings when silicon content is low (4 at.%) and these clusters disappeared at a high silicon content.

DOI: 10.5963/AMSA0401001

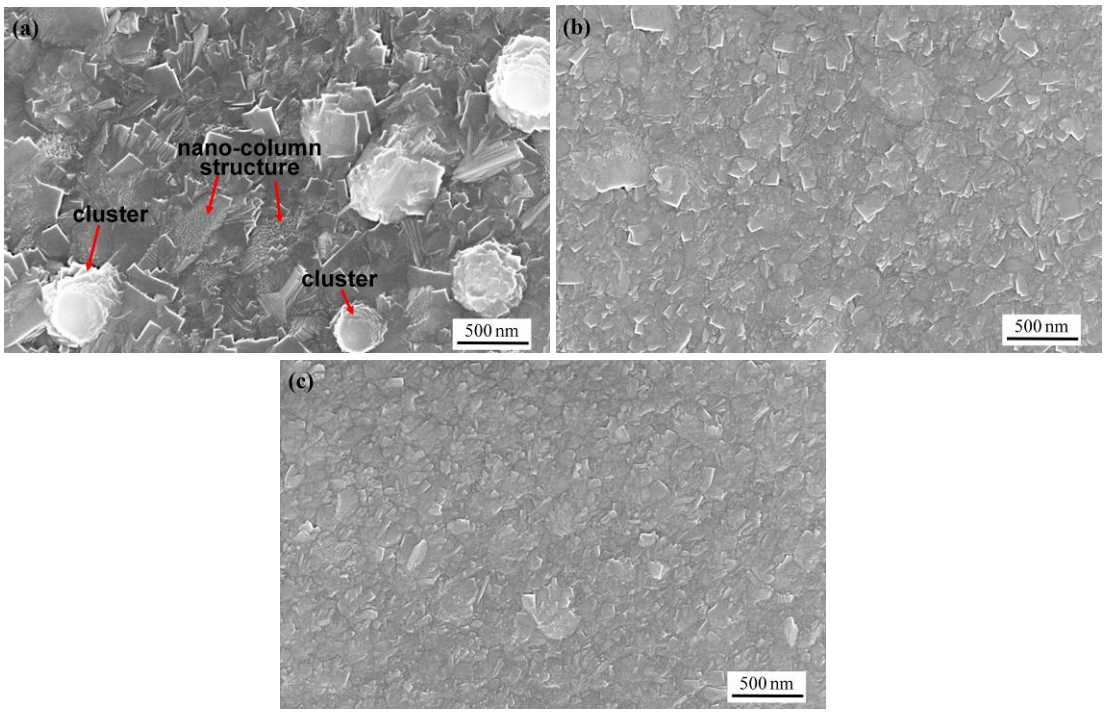

Fig. 6 SEM photos of TiAlSiN coatings with different silicon contents: (a) silicon content = 4 at.%, (b) silicon content = 6 at.%, (c) silicon content = 8 at.%

Fig. 6(a) shows that the lamellar structure at the surface of TiAlSiN coatings are actually composed by rather small nano-column structure. And these small nano-column structure may be the main reason for a strong (111) orientation TiAlSiN coating in the XRD results. When increasing the silicon content from 4 at.% to 6 at.%, these small nano-column structures are almost disappeared, which results in a sharp decrease of (111) intensity. This phenomenon means that the growth mode changes from columnar growth [18, 19] to nanocrystals growth.

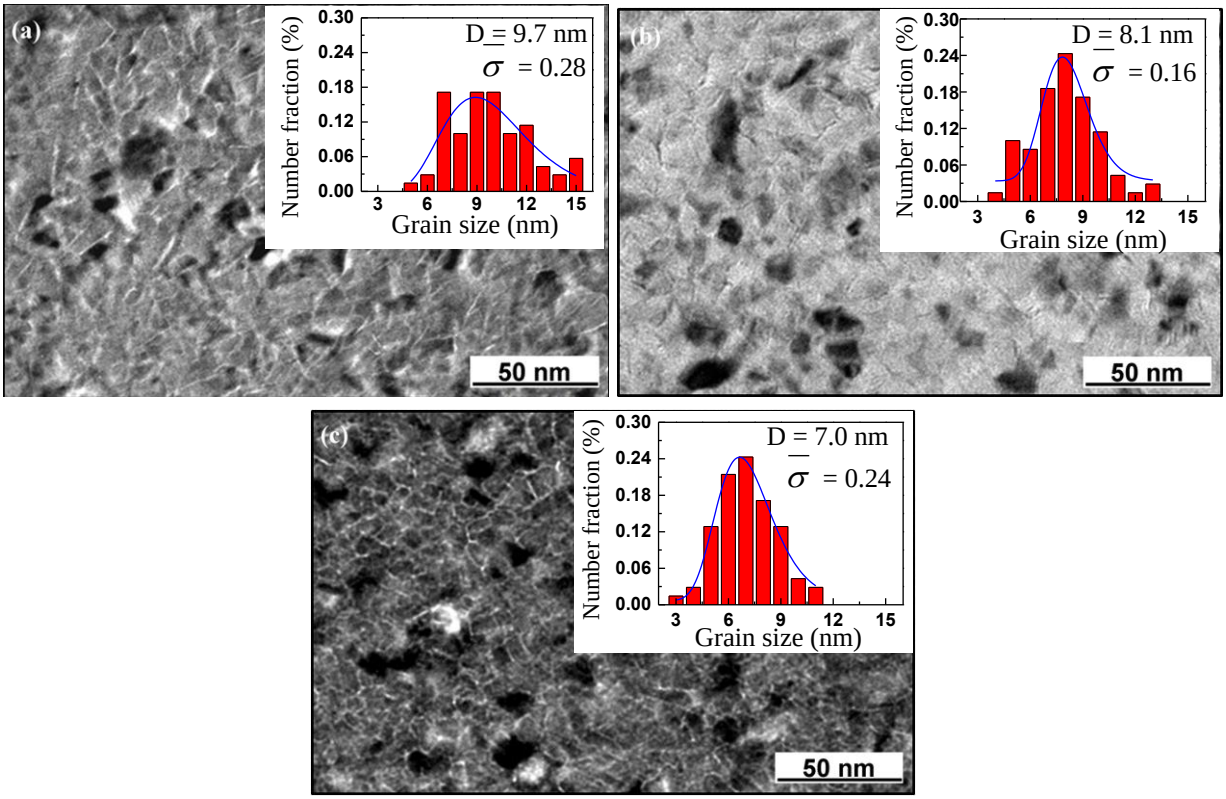

Fig. 7 TEM images and particle size distribution of TiAlSiN coatings with different silicon contents: (a) silicon content = 4 at.%, (b) silicon content = 6 at.%, (c) silicon content = 8 at. %

The TEM images of TiAlSiN coatings are shown in Fig. 7. With increasing silicon content, the average grain size decreases. The particle size distribution histogram shown in Fig. 7 was obtained after a statistical analysis of the grain size, where D is the

DOI: 10.5963/AMSA0401001

average gain size and $\bar{\sigma}$ is standard deviation. It can clearly be seen that the grain size of TiAlSiN is refined to 7.0 nm at the silicon content = 8 at.%. And the distribution of grain size becomes more concentrated with increasing silicon content.

D. Hardness and Adhesion

Results of the nanoindentation tests are shown in Fig. 8. The nanoindentation test results exclude some abnormal data points by two principles. One is the irregular shape (not equilateral triangle shape) of indentation observed by scanning electron microscopy. The other is the data deviated from other hardness values largely. A commercialized turning insert KC5510 produced by Kennametal Inc was also characterized using the same method in order to compare with the TiAlSiN coatings experienced in this work. There are two reasons for choosing KC5510. Firstly, KC5510 is a TiAlN coating prepared by PVD method. Therefore, we can investigate the effect of the introduction of the silicon element to the hardness of coatings roughly. Secondly, since the thickness of KC5510 is close to the thickness of TiAlSiN coatings (approximately 3 μm) of the current work; this can avoid the thickness influence on the hardness results of the coatings [20].

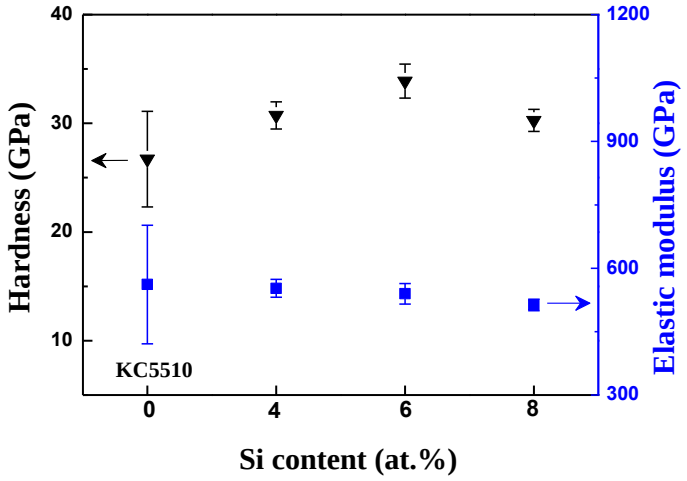

Fig. 8 Hardness of TiAlSiN coatings with the change of Si content tested by nanoindentation

Fig. 8 shows that the hardness of all TiAlSiN coatings exceeds 30 GPa. The introduction of the silicon element can increase the hardness; and the relationship between hardness and silicon content is nonlinear. This may be explained by a hybrid hardening mechanism, which is the interaction of different mechanisms of hardening. When the silicon content is low (4 at.%), the introduction of silicon element can refine the grain while producing solid solution strengthening. So, the hardness of TiAlSiN coating has a large improvement over the hardness of TiAlN coating. When the silicon content increases to 6 at.%, a further increase in hardness may be due to the formation of a better nanocrystal/amorphous structure. This nanocomposite structure (nanocrystal / amorphous structure) can strongly inhibit the movement of dislocations to achieve high hardness [14, 21-24]. By continuing increase in the silicon content to 8 at.%, although the grain size becomes smaller, the hardness decreased slightly. This may be due to the excessive existence of the amorphous phase at grain boundaries. The excessive existence of the amorphous phase will weaken the effect of grain boundary strengthening.

Tsui et *al.* [25] proposed that the resistance to plastic deformation of a hard coating is proportional to H^3/E^2; where H is the indentation hardness and E is the Young's modulus. As it can be seen from Fig. 9 that when the silicon content is 6 at.%, the H^3/E^2 value is the highest, which means that a good plastic deformation resistance and a promising application in modern machining.

DOI: 10.5963/AMSA0401001

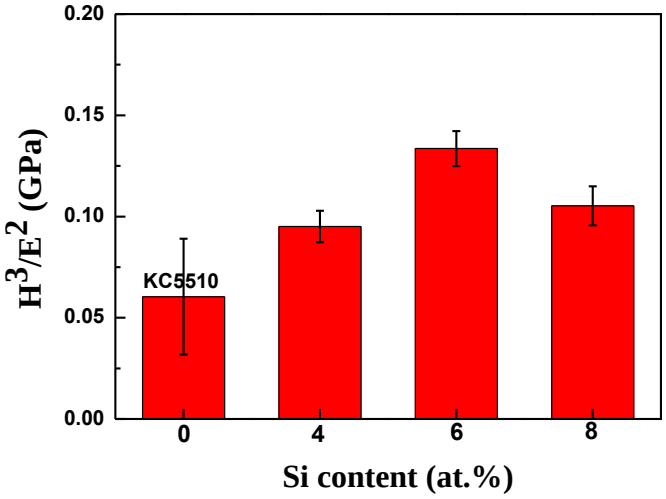

Fig. 9 H^3/E^2 values of TiAlSiN coatings with different silicon contents

The results of the scratching tests are summarized in Fig. 10. The larger the critical load value, the higher the bonding strength of the coating and the substrate. The dash line in Fig. 10 represents the critical load value of three kinds of hard tool coating [12, 26, 27]. Among these coatings, TiN coating in [26] is a commercial product produced by Mitsubishi Corporation. It can be seen that the critical load values of all TiAlSiN coatings are good; all the values exceed 60 N. It can be found that low silicon content is beneficial to binding force, which can be attributed to a strong (111) preferred orientation.

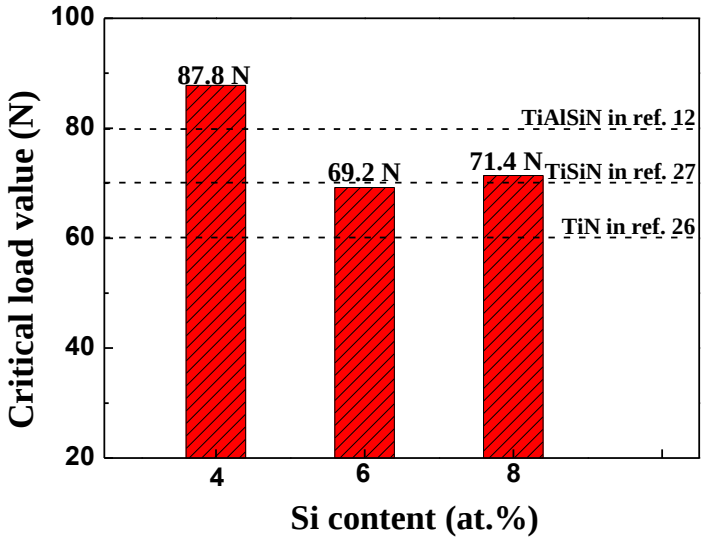

Fig. 10 Critical load values of TiAlSiN coatings with different silicon contents

IV. CONCLUSIONS

The main conclusions reached in this work are listed as follows:

(1) All peaks of coatings were shown to be the NaCl structure of TiAlN phase. No peaks related with nitrides of Al and silicon was detected. The TiAlSiN coating is proved to be composed by nanocrystalline TiAlN or TiAlSiN and amorphous Si_3N_4 according to XRD and XPS results.

(2) With increasing the silicon content from 4 at.% to 8 at.%, the grain size of TiAlSiN coatings is refined to 7.0 nm and distributes more concentrated. Moreover, the nano-column structure at the TiAlSiN coating surface almost disappears in this process, which may mean that the growth mode changes from columnar growth to nanocrystals growth.

(3) The hardness and silicon content showed a nonlinear relationship, which may be explained by a hybrid hardening mechanism. The highest hardness is obtained at 6 at.% silicon, as it owes a relatively good nanocomposite structure (nanocrystal/amorphous) and relatively fine grains (8.1 nm).

DOI: 10.5963/AMSA0401001

(4) TiAlSiN coating with 4 at.% silicon content has the highest critical load of 87.8 N, which means a strong (111) preferred orientation is good for the adhesion strength. As the silicon content increases, the preferred orientations changed from (111) to (200) and the adhesion strength decreases.

(5) The optimized mechanical properties of the TiAlSiN coatings, with a nanohardness of about 33.8 GPa and a critical load of 69.2 N, were prepared by using a TiAlSi alloy target with 6 at.% silicon content.

ACKNOWLEDGMENTS

The authors gratefully acknowledge the financial support of the National Science and Technology Major Project (2012ZX04003061).

REFERENCES

[1] S. Pervaiz, A. Rashid, I. Deiab, and M. Nicolescu, "Influence of tool materials on machinability of titanium- and nickel-based alloys: a review," *Materials and Manufacturing Processes*, vol. 29, iss. 3, pp. 219-252, 2014.

[2] B. Yang, L. Chen, K. K. Chang, W. Pan, Y. B. Peng, Y. Du, and Y. Liu, "Thermal and thermo-mechanical properties of Ti-Al-N and Cr-Al-N coatings," *International Journal of Refractory Metals and Hard Materials*, vol. 35, pp. 235-240, 2012.

[3] Z. Q. Liu, J. X. An, J. Y. Xu, and M. Chen, "Wear performance of (nc-AlTiN)/(a-Si3N4) coating and nc-AlCrN)/(a-Si3N4) coating in high-speed machining of titanium alloys under dry and minimum quantity lubrication (MQL) conditions," *Wear*, vol. 305, pp. 249-259, 2013.

[4] D. G. Thakur, B. Ramamoorthy, and L. Vijayaraghavan, "Some investigations on high speed dry machining of aerospace material inconel 718 using multicoated carbide inserts," *Materials and Manufacturing Processes*, vol. 27, iss. 7, pp. 1066-1072, 2012.

[5] G. Z. Wu, S. L. Ma, K. W. Xu, V. Ji, and P. K. Chu, "Oxidation resistance of quintuple Ti-Al-Si-C-N coatings and associated mechanism," *Journal of Vacuum Science and Technology A*, vol. 30, iss. 4, pp. 041508-041508-9, 2012.

[6] H. C. Barshilia, M. Ghosh, R. Shashidhara, and K. S. Ramakrishna, "Deposition and characterization of TiAlSiN nanocomposite coatings prepared by reactive pulsed direct current unbalanced magnetron sputtering," *Applied Surface Science*, vol. 256, iss. 21, pp. 6420-6426, 2010.

[7] S. Carvalho, N. M. G. Parreira, M. Z. Silva, A. Cavaleiro, and L. Rebouta, "In-service behaviour of (Ti,Si,Al)NX nanocomposite films," *Wear*, vol. 274-275, pp. 68-74, 2012.

[8] S. Veprek and S. Reiprich, "A concept for the design of novel superhard coatings," *Thin Solid Films*, vol. 268(1), iss. 1-2, pp. 64-71, 1995.

[9] S. Carvalho, E. Rebouta, F. Vaz, and D. Schneider, "Elastic properties of (Ti,Al,Si)N nanocomposite films," *Surface & Coatings Technology*, vol. 142, pp. 110-116, 2001.

[10] S. M. Yang, Y. Y. Chang, and D. Y. Lin, "Thermal stability of TiAlN and nanocomposite TiAlSiN thin films," *Journal of Nanoscience and Nanotechnology*, vol. 9, iss. 2, pp. 1108-1112, 2009.

[11] Z. W. Xie, L. P. Wang, and X. F. Wang, "Influence of oxidation on the structural and mechanical properties of TiAlSiN coatings synthesized by multi-plasma immersion ion implantation and deposition," *Nuclear Instruments and Methods in Physics Research B*, vol. 271, pp. 1-5, 2012.

[12] D. H. Yu, C. Y. Wang, and X. L. Cheng, "Microstructure and properties of TiAlSiN coatings prepared by hybrid PVD technology," *Thin Solid Films*, vol. 517, iss. 17, pp. 4950-4955, 2009.

[13] D. Philippon, V. Godinho, and P. M. Nagy, "Endurance of TiAlSiN coatings: Effect of Si and bias on wear and adhesion," *Wear*, vol. 270, iss. 7-8, pp. 541-549, 2011.

[14] L. Chen, J. Paulitsch, Y. Du, and P. H. Mayrhofer, "Thermal stability and oxidation resistance of Ti-Al-N coatings," *Surface & Coatings Technology*, vol. 206, iss. 11-12, pp. 2954-2960, 2012.

[15] J. M. Castanho and M. T. Vieira, "Effect of ductile layers in mechanical behaviour of TiAlN thin coatings," *Journal of Materials Processing Technology*, vol. 143-144, pp. 352-357, 2003.

[16] C. L. Chang, J. W. Lee, and M. D. Tseng, "Microstructure, corrosion and tribological behaviors of TiAlSiN coatings deposited by cathodic arc plasma deposition," *Thin Solid Films*, vol. 517, iss. 17, pp. 5231-5236, 2009.

[17] M. Diserens, J. Patscheider, and F. Levy, "Improving the properties of titanium nitride by incorporation of silicon," *Surface & Coatings Technology*, vol. 108, iss. 1-3, pp. 241-246, 1998.

[18] S. Q. Wang, L. Chen, B. Yang, K. K. Chang, Y. Du, J. Li, and T. Gang, "Effect of Si addition on microstructure and mechanical properties of Ti-Al-N coating," *Int. Journal of Refractory Metals and Hard Materials*, vol. 28, iss. 5, pp. 593-596, 2010.

[19] E. Altuncu and F. Ustel, "Correlation between sputtering conditions and growth properties of (TiAl)N/AlN multilayer Coatings," *Materials and Manufacturing Processes*, vol. 24, iss. 7-8, pp. 796-799, 2009.

[20] V. G. Sargade, S. Gangopadhyay, S. Paul, and A. K. Chattopadhyay, "Effect of coating thickness on the characteristics and dry machining performance of TiN film deposited on cemented carbide inserts using CFUBMS," *Materials and Manufacturing Processes*, vol. 26, iss. 8, pp. 1028-1033, 2011.

[21] A. A. Voevodin and J. S. Zabinski, "Supertough wear-resistant coatings with 'chameleon' surface adaptation," *Thin Solid Films*, vol. 370, iss. 1-2, pp. 223-231, 2000.

[22] J. S. Koehler, "Attempt to design a strong solid," *Physical Review B*, vol. 2, pp. 547-551, 1970.

DOI: 10.5963/AMSA0401001

[23] S. Carvalho, L. Rebouta, E. Ribeiro, F. Vaz, M. F. Denannot, and J. Pacaud, "Microstructure of (Ti,Si,Al)N nanocomposite coatings," *Surface and Coatings Technology*, vol. 177, pp. 369-375, 2004.

[24] V. Godinho, T. C. Rojas, and S. Trasobares, "Microstructural and chemical characterization of nanostructured TiAlSiN coatings with nanoscale resolution," *Microscopy and Microanalysis*, vol. 18, iss. 3, pp. 568-581, 2012.

[25] T. Y. Tsui, W. C. Pharr, C. S. Oliver, and R. L. Bhatia, "Nanoindentation and nanoscratching of hard carbon coatings for magnetic disks," *Materials Research Society Symposium Proceedings*, vol. 383, pp. 447-452, 1995.

[26] http://www.mitsubishicarbide.net/contents/mmsc/zh/html/product/technical_information/grade/milling/co_violet.html.

[27] F. Vaz, L. Rebouta, S. Ramos, A. Cavaleiro, M. F. da Silva, and J. C. Soares, "Physical and mechanical properties of Ti1-xSixN films," *Surface and Coatings Technology*, vol. 100-101, iss. 1-3, pp. 110-115, 1998.

DOI: 10.5963/AMSA0401001